

Crystallinity and fusion of low molecular weight α, ω -alkoxy-poly(ethylene oxide): methoxy to octadecoxy end-groups

D. R. Cooper, Y.-K. Leung, F. Heatley and C. Booth

Department of Chemistry, University of Manchester, Manchester M13 9PL, UK

(Received 5 September 1977)

Samples of α, ω -alkoxy-poly(ethylene oxide) with oxyethylene inner blocks of 70 to 150 chain atoms and end blocks ranging from C₁ (methoxy) to C₁₈ (octadecoxy) have been prepared and characterized. Several experimental methods have been used to investigate their crystalline structure and melting behaviour. The polymers crystallize into stacked structures in which crystalline and non-crystalline layers alternate. The methylene chains are in the non-crystalline layers together with a significant fraction (about 0.2) of the oxyethylene inner block. The crystalline layers contain extended or folded oxyethylene chains, depending upon the relative lengths of the inner and end blocks. The melting points either are roughly independent of methylene block length (extended-chain crystals) or increase with methylene block length (folded-chain crystals). This melting behaviour is explained by a combination of two important effects: conformational restriction of the cilia emerging into the non-crystalline layer and mixing of the methylene and oxyethylene chains in the melt.

INTRODUCTION

The crystallization of low molecular weight α, ω -hydroxy-poly(ethylene oxide), and the morphology and melting of the solids so obtained, has been extensively studied¹⁻⁹. The stacked lamella structure of the solid is particularly well defined: several orders of Bragg scattering can be observed by small-angle X-ray scattering¹⁻⁴ and Raman scattering from the longitudinal acoustic mode of the helix in the crystal is also prominent^{10,11}. Within the crystalline lamellae the poly(ethylene oxide) chains are folded to an extent which depends upon the chain length and the crystallization temperature^{2-5,9,10}: samples of molecular weight less than $\bar{M}_n = 3000$, crystallized above room temperature, have essentially unfolded (extended chain) structures.

From similar, though less extensive, investigations of low molecular weight poly(ethylene oxide) fractions with other end-groups¹²⁻¹⁶ it appears that the predominant determining factor for the structure is the chain length (at least for the samples of narrow chain length distribution used in crystallization studies). In other words, such changes in properties as are attributable to end-group effects do not significantly disturb the overall pattern of results which has been established for hydroxy-ended polymers.

Block copolymers containing poly(ethylene oxide) have also been investigated with respect to their crystallization and crystallinity. We have shown¹⁷⁻¹⁹ that the properties of oxyethylene-oxypropylene diblock (PE) and triblock (PEP) copolymers relate to those of poly(ethylene oxide) homopolymers. In that these block copolymers necessarily crystallize into structures containing alternating crystalline and non-crystalline layers they form useful models for investigating the bulk crystallized state of polymers.

In this paper we report the preparation and properties of α, ω -alkoxy-poly(ethylene oxide) samples with end-groups

ranging from C₁ (methoxy) to C₁₈ (octadecoxy). These compounds form a bridge between what are conventionally regarded as homopolymers and what might be thought of as methylene-oxyethylene block copolymers (MEM). In a subsequent paper we hope to report on similar samples with end-groups longer than C₂₀.

EXPERIMENTAL AND RESULTS

Preparation

A modified²⁰ Williamson ether synthesis was used to prepare α, ω -alkoxy-poly(ethylene oxide) from α, ω -hydroxy-poly(ethylene oxide) samples of molecular weight (\bar{M}_n) 1000 and 1500 (Shell Chemical Co. Ltd.) and 2000 (Hoechst Chemicals Ltd.). Preparative details are given in Appendix I.

Notation

We denote samples by their number-average block lengths, expressed in oxyethylene or methylene chain units as appropriate: thus α, ω -heptoxy-poly(ethylene oxide) prepared from poly(ethylene oxide) 2000 is labelled 7-45-7. We prepared two sets of samples from poly(ethylene oxide) 2000. In tabulating results we refer to these as preparations A and B.

Characterization

Infra-red spectroscopy was used as described earlier²⁰ to determine conversions of hydroxy to alkoxy of better than 97%. Low frequency (720-765 cm⁻¹) absorptions, assigned to rocking motions of the alkoxy end-groups, were observed for all samples with end-groups longer than C₂. End-group analysis (phthaloylation in pyridine) was used to confirm the infra-red estimates of the conversions. No trace of iodine could be detected by elemental analysis or by heating the

Table 1 Molecular characteristics

Sample	\bar{M}_n (g/mol)			\bar{M}_w/\bar{M}_n
	Predicted	V.p.o.	G.p.c.	G.p.c.
0-23-0	1000	980	1000	1.06
1-23-1	1028	980	1000	1.05
2-23-2	1056	—	1000	1.05
3-23-3	1084	—	1120	1.06
4-23-4	1112	—	1150	1.06
7-23-7	1196	1230	1270	1.06
10-23-10	1280	—	1350	—
12-23-12	1336	—	1400	1.07
16-23-16	1448	—	1600	—
18-23-18	1504	—	1650	—
0-34-0	1500	—	1490	1.04
1-34-1	1528	—	1490	1.05
2-34-2	1556	—	1510	1.04
3-34-3	1584	—	1560	—
4-34-4	1612	—	1600	—
7-34-7	1696	—	1700	—
10-34-10	1780	—	1800	—
12-34-12	1836	—	1850	—
16-34-16	1948	—	2050	—
18-34-18	2004	—	2100	—
			A ^a B ^a	
0-45-0	2000	1980	2000 2000	1.06
1-45-1	2028	1980	2000 2000	1.04
2-45-2	2056	2000	2000 2040	1.05
3-45-3	2084	—	— 2050	1.06
4-45-4	2112	—	2100 2080	1.06
7-45-7	2196	2200	2250 2210	1.06
10-45-10	2280	—	2300 2330	1.07
12-45-12	2336	—	2400 2370	1.06
16-45-16	2448	—	2500 2410	1.07
18-45-18	2504	—	2600 2530	1.08

^aResults for preparations A and B. All other results (v.p.o., \bar{M}_w/\bar{M}_n) for the 45 series are for preparation B

samples with silver nitrate in a mixture of methanol and nitric acid.

Number-average molecular weights (\bar{M}_n) were measured by vapour pressure osmometry (v.p.o., Mechrolab, benzene at 25°C). Number-average molecular weights were also determined from the elution volume in gel permeation chromatography (g.p.c., tetrahydrofuran at 25°C) by comparison with the elution volumes of standard samples. Details of the conditions for g.p.c. are given elsewhere²¹. A complete analysis of the g.p.c. data was not carried out for every sample. Values of \bar{M}_n and of \bar{M}_w/\bar{M}_n (where appropriate) are given in Table 1. The values of \bar{M}_n are in good agreement with those predicted (Table 1) from the manufacturer's molecular weights of the original poly(ethylene oxide) samples*. The values of \bar{M}_w/\bar{M}_n are essentially unchanged by alkoxylation.

X-ray scattering

Wide-angle X-ray scattering (WAXS) photographs (Debye-Scherrer camera, CuK α radiation) of selected samples (1-23-1, 12-23-12, 1-45-1, 18-45-18) crystallized at 25°C

* The close agreement between the g.p.c. results on the one hand and the v.p.o. and predicted results on the other, implies that, in tetrahydrofuran at 25°C, the contribution of the methylene chain to the hydrodynamic volume is roughly equivalent to that of an equal mass of oxyethylene chain. This is consistent with the solubility parameter of tetrahydrofuran being about halfway between those of polyethylene and poly(ethylene oxide)²².

were identical, except for the amorphous background, one with another and with photographs of the poly(ethylene oxide) homopolymers. It is concluded that the alkyl chains do not crystallize in these samples.

Small-angle X-ray scattering (SAXS) photographs (Rigaku-Denki slit collimated camera, CuK α radiation¹⁸) of the solid polymers, crystallized at 25°C, were similar to those reported previously for poly(ethylene oxide) homopolymers¹⁻⁴ and block copolymers¹⁷⁻¹⁹. Lamella spacings (l_x), calculated by direct use of Bragg's Law, are listed in Table 2. For comparison the lengths of the extended chains (l) are also given: we take the length of an oxyethylene chain unit to be 0.28 nm and that of a methylene chain unit to be 0.125 nm²². Results obtained for samples crystallized at 35°C differed insignificantly from those for samples crystallized at 25°C; however, certain samples crystallized at 45°C showed significantly different photographs. Two sets of Bragg peaks were observed for samples 0-23-0 and 1-23-1 (and also for sample 2-23-2 crystallized at 35°C); this observation is attributable to fractionation during the crystallization process¹. Broad peaks were observed for samples with long ($\geq C_{16}$) alkoxy end-groups.

The SAXS results (Table 2) show that crystallization at 25°C leads to extended-chain structures for polymers with short methylene chains and to folded-chain structures for polymers with long methylene chains for all three series. The methylene chain length (n) at which the transition from extended to folded-chain structure occurs, varies with the oxyethylene block length (E) roughly as follows: $E = 23$, $n \leq 16$; $E = 34$, $n \leq 12$; $E = 45$, $n = 7$. The significant effect of crystallization temperature (T_c) on the spacings is illus-

Table 2 Small-angle X-ray and Raman scattering^a

Sample	Approximate chain length l (nm)	Lamella spacing l_x (nm)	Raman frequency $\bar{\nu}_1$ (cm ⁻¹)
0-23-0	6.4	7.6, 6.6	—
1-23-1	6.7	7.7, 6.7	—
2-23-2	6.9	7.6	—
3-23-3	7.2	7.6	—
4-23-4	7.4	7.8	—
7-23-7	8.2	8.3	—
12-23-12	9.4	8.7	—
16-23-16	10.4	7.3	—
18-23-18	10.9	7.9; 11.2 ^b	—
0-34-0	9.5	9.5	—
1-34-1	9.8	10.1	—
2-34-2	10.0	10.1	—
12-34-12	12.5	8.1	—
16-34-16	13.5	8.6	—
18-34-18	14.0	8.9; 8.8, 14.3 ^b	—
		A B B	
0-45-0	12.6	— 13.2	9.0
1-45-1	12.9	13.3	13.8 8.3
2-45-2	13.1	13.7	14.0 8.3
3-45-3	13.4	—	14.0 7.5
4-45-4	13.6	14.1	14.1 7.5
7-45-7	14.4	—	8.9 7.5, 12.0
10-45-10	15.1	9.5	8.9 11.5
12-45-12	15.6	—	9.3 11.5
16-45-16	16.6	—	9.5 11.0
18-45-18	17.1	10.6; 11.2 ^b	9.6 11.0

^aFor samples crystallized at $T_c = 25^\circ\text{C}$ except where noted;

^b $T_c = 45^\circ\text{C}$

Table 3 Specific volumes (v_{sp}) at 25°C of samples crystallized at 25°C and calculated volume changes on crystallization (Δv)

Sample	v_{sp} (cm ³ /g)	Δv (cm ³ /g of oxyethylene)
0-23-0	0.832	0.059
1-23-1	0.835	0.066
2-23-2	0.845	0.066
3-23-3	0.852	0.067
4-23-4	0.868	0.059
7-23-7	0.876	0.073
12-23-12	0.912	0.063
B		
0-45-0	0.822	0.069
1-45-1	0.837	0.059
2-45-2	0.835	0.066
3-45-3	0.845	0.060
4-45-4	0.846	0.064
7-45-7	0.874	0.047
10-45-10	0.890	0.042
12-45-12	0.893	0.047
16-45-16	0.899	0.056
18-45-18	0.909	0.051

trated by the results obtained for the samples with octadecyloxy end-groups crystallized at $T_c = 25^\circ$ and 45°C (Table 2).

SAXS was also used to examine the melts of certain samples. Films of molten polymer (thickness ~ 1 mm) were enclosed in thin Melinex polyester films in a Rigaku-Denki fibre specimen holder held at $63 \pm 1^\circ\text{C}$ and exposed to CuK α radiation in a Rigaku-Denki slit collimated goniometer. The intensity of scattered radiation was measured by use of a Phillips scintillation detector system. The scattering envelopes from samples 0-23-0, 12-23-12, 0-45-0, 7-45-7 and 18-45-18 were practically identical one with another. Thus we find *no evidence* from SAXS to support the view that the melts of any of our samples are inhomogeneous.

Raman scattering

Raman spectra were obtained, as described elsewhere^{10,11} for series 45. Samples of series 23 and 34 were not investigated by this method; results for the α,ω -hydroxy-polymers have been given elsewhere¹⁰. The fundamental frequencies ($\bar{\nu}_1$) of the longitudinal acoustic modes of vibration of the lamellae are listed in Table 2. These results confirm the conclusions drawn from the SAXS experiments, and show explicitly the two types of lamellae (extended and folded) present in sample 7-45-7 crystallized at 25°C . For a given type of crystal the fall in $\bar{\nu}_1$ with increasing length of the alkoxy end-group is indicative of the effect of the non-crystalline components of stacked lamella structures on the longitudinal acoustic vibration^{11,23}.

Picnometry

Specific volumes at 25°C (v_{sp}) of the solid polymers, crystallized at 25°C , were determined by picnometry as described elsewhere¹⁸. Results are given in Table 3: reproducibility was ± 0.003 cm³/g. The increase in v_{sp} with increased length of the methylene chain is due mainly to the increased proportion of non-crystalline material in the solid. A better presentation of the results is as Δv , the change in volume on crystallization at 25°C per gram of oxyethylene. This can be calculated, assuming additivity of volumes in the supercooled melt, from the known specific volumes of the oxyethylene chain (0.891 cm³/g)²⁴ and the methylene chain (1.182 cm³/g)²⁵. For a given type of crystal (extended-chain, folded-chain) Δv is seen to be constant: the scatter of

results is a consequence of the imprecision of the method of measuring v_{sp} for small samples. The values found for Δv are about 0.064 cm³/g for extended-chain crystallization and about 0.049 cm³/g for folded-chain crystallization. These values are to be compared with $\Delta v^0 = 0.075$ cm³/g which can be calculated for the perfect crystallization of poly(ethylene oxide) from the specific volume, 0.816 cm³/g, of perfectly crystalline poly(ethylene oxide) at 25°C found from WAXS experiments²².

Differential scanning calorimetry

Specific heats of fusion at the melting temperature [$\Delta h_{sp}(T_m)$] of the solid polymers, crystallized at 25°C , were determined from endotherm peak areas obtained by differential scanning calorimetry (d.s.c., Perkin-Elmer DSC-2). The heating rate selected was 2.5 K/min. The calorimeter was calibrated daily by melting indium.

Samples 0-23-0, 1-23-1 and 2-23-2 showed multi-peaked endotherms which are attributable to fractionation during the crystallization process¹ (see SAXS results). Sample 7-45-7 showed two distinct endotherms due to the presence of extended-chain and folded-chain structures (see SAXS and Raman results). The folded-chain crystals (lower melting) contribute about 75% of the heat of fusion of the sample crystallized at 25°C . This proportion is independent of the heating rate (0.6 to 5.0 K/min) and so the folded form can be categorized⁹ as kinetically stable. The thickness of this kinetically stable lamella (22 oxyethylene chain units, 6.5 nm) is very much smaller than the minimum thickness of stable folded lamellae formed from α,ω -hydroxy-poly(ethylene oxide)⁹. We noted in preliminary d.s.c. experiments that the folded chain crystals formed at 25°C from samples 16-23-16, 18-23-18, 12-34-12, 16-34-16 and 18-34-18 were kinetically unstable.

The other samples investigated showed single-peaked endotherms. Specific heats of fusion could be derived with a reproducibility of ± 5 J/g. Values of $\Delta h_{sp}(T_m)$ are listed in Table 4. Also listed are values of $\Delta h(54^\circ\text{C})$, the heat of fusion per gram of oxyethylene corrected to constant temperature (54°C) by using $C_p \sim 0.7$ J/K g²⁶. For a given type of crystal $\Delta h(54^\circ\text{C})$ is seen to be constant; the values found are about 170 J/g for extended-chain crystals and about 140 J/g for folded-chain crystals. These values are to be compared with a value of $\Delta h^0 = 200$ J/g (corresponding to 210 J/g at

Table 4 Heats of fusion of samples crystallized at 25°C

Sample	$\Delta h_{sp}(T_m)$ (J/g)	$\Delta h(54^\circ\text{C})$ (J/g of oxyethylene)
3-23-3	163	167
4-23-4	158	165
7-23-7	148	166
12-23-12	135	175
B		
0-45-0	171	171
1-45-1	171	173
2-45-2	171	176
3-45-3	163	169
4-45-4	164	172
7-45-7	149	158
10-45-10	140	141
12-45-12	126	140
16-45-16	120	141
18-45-18	118	144

Table 5

Sample	Melting points ^a , T_m (°C)			
	D.s.c.	Dilatometry	Microscopy	
			Reichert	Low C_p
0-23-0	—	38.4 ^b	—	—
1-23-1	—	37.4 ^b	37.2	—
2-23-2	—	40.0 ^b	—	39.6
3-23-3	40.5	—	39.3	38.9
4-23-4	40.3	39.9 ^c	39.1	38.2
7-23-7	40.6	—	39.2	38.4
10-23-10	—	—	39.7	—
12-23-12	42.3	—	42.1	41.8
18-23-18	—	53.9 ^d	—	—
0-34-0	—	47.8 ^b	—	—
1-34-1	—	47.4 ^b	—	—
2-34-2	—	47.9 ^b	48.2	—
3-34-3	—	—	48.1	—
4-34-4	—	—	47.5	—
7-34-7	—	—	45	—
10-34-10	—	—	45	—
18-34-18	—	47.7, 53–55 ^d	47	—
	B	A	A	B
0-45-0	53.6 ^e	53.6 ^b	53.6	—
1-45-1	52.4	53.2 ^b	53.4	52.6
2-45-2	53.2	53.8 ^b	53.8	53.7
3-45-3	52.3	—	—	52.8
4-45-4	52.4	52.7 ^d	52.2	53.0
7-45-7	42.8, 47.0	—	—	—
10-45-10	43.1	—	43.3	43.6
12-45-12	—	—	44.0	43.8
16-45-16	46.5	—	48.2	45.1
18-45-18	48.9	—	50.4	47.8

^aFor samples crystallized at $T_c = 25^\circ\text{C}$ except where noted;

^bData from ref. 16; ^c $T_c = 35^\circ\text{C}$; ^d $T_c = 45^\circ\text{C}$; ^eCalibrant for d.s.c.

68°C^{27} for the heat of fusion of perfectly crystalline poly(ethylene oxide)[†],

Melting points (T_m) of the solids, crystallized at 25°C , were determined by d.s.c. from the endotherm peak positions; the temperature scale of the calorimeter was checked daily for linearity and was calibrated against sample 0-45-0 ($T_m = 53.6^\circ\text{C}$). Measurements were made at several heating rates and also extrapolations were made to zero heating rate. Within the reproducibility of results ($\pm 0.5\text{K}$) there was no difference between values of T_m obtained at zero and at 2.5 K/min. Melting points are given in Table 5.

Dilatometry

Melting points were determined by dilatometry following the procedures described elsewhere¹⁸. Melting points, defined as the temperature of disappearance of the last trace of crystallinity, are listed in Table 5. Dilatometric melting points were independent of T_c within the ranges $T_c = 25^\circ$ to 35°C (series 23 and 34) and $T_c = 35^\circ$ to 45°C (series 45).

The dilatometric results for sample 18-34-18 are interesting since the sample, crystallized at 25°C , melted completely at 47.7°C at a heating rate of 6 K/h and then slowly recrystallized when held at temperatures about 47° or 50°C . The solids so formed melted at 53.4°C ($T_c \sim 47^\circ\text{C}$) or 55.1°C ($T_c \sim 50^\circ\text{C}$). It seems that sample 18-34-18 is an example

[†] Devoy's value of Δh_{sp} (68°C)²⁷ was obtained from measurement of the melting point depression of high molecular weight poly(ethylene oxide) by an added solvent. The method is described elsewhere²⁸.

of a material in which recrystallization in extended-chain form of unstable folded-chain crystals is sufficiently slow to be studied most easily by dilatometry.

Optical microscopy

Melting points of the solid polymers were determined on the hot stage of a polarizing microscope. Samples were crystallized at $T_c = 25^\circ$ or 35°C . A wide variety of crystalline morphologies were apparent (spherulitic, dendritic, fibrillar, etc.); no attempt was made to record these in detail since, for many samples, the morphology was markedly dependent on the crystallization conditions. Two methods were used. In early measurements a Reichert hot stage polarizing microscope was used at a heating rate of 1 K/min to determine approximate melting points ($\pm 0.5\text{K}$). In later measurements a hot stage of low heat capacity regulated (to $\pm 0.01\text{K}$) by a proportional heater and capable of a controlled heating rate of 2 K/sec was employed. Samples were crystallized at 25° or 35°C and then rapidly heated to a temperature 2K below T_m before traversing the melting region at 0.1 K/min. This procedure avoided complications of premelting and recrystallization. Calibration was by eight melting point standards in the range 35° to 68°C . Results are given in Table 5, melting points being defined as the temperature of disappearance of the last trace of birefringence. The melting points of samples crystallized at 35°C differed insignificantly from those of samples crystallized at 25°C . Few results are quoted for the unstable folded-chain crystals of series 23 and series 34 because of difficulty in quantifying the gradual changes in birefringence which were observed.

Nuclear magnetic resonance

Proton magnetic resonance spectra of the solid polymers of series 45, crystallized at 25°C , were recorded at 20°C by means of a Varian Associates SC-300 spectrometer operating in continuous wave mode at 300 MHz. Selected spectra are illustrated in Figure 1: the spectra are sensitive to traces of impurity and differed in detail, but not in a significant way, between the two preparations. A broad peak is associated with immobile protons and a 'narrow peak' with mobile protons situated, presumably, in the disordered layers. The narrow peak in Figures 1b–1e is just resolved into two components separated by ~ 2 ppm corresponding to oxyethylene protons (lower shielding) and methylene protons (higher shielding), showing that the disordered layers are a mixture of oxyethylene and methylene chains.

The fraction of mobile protons (p), assessed as the ratio of the area under the narrow peak to that under the broad peak, is listed for each of the samples of preparation B in Table 6. (The results for preparation A are identical within ± 0.02 .) Even allowing for the large error in p (± 0.02) arising from the difficulty of clearly separating the broad and narrow peaks, the mobile fractions for the longer methylene end blocks are significantly lower than those expected if all methylene protons are mobile. Judging by the tendency of p to approach an asymptote of ~ 0.1 , corresponding to about 20 mobile protons, as the alkyl chain length increases, it seems likely that only protons on the last two or three alkyl carbon atoms are sufficiently mobile to give a peak as narrow as the mobile oxyethylene component. Further work is in progress on this point.

Proton and ^{13}C spin lattice relaxation times (T_1) of molten samples 7-45-7 and 18-45-18 and of molten octadecane were measured by means of a Varian Associates XL-100 spectrometer by the (π - τ - $\pi/2$) inversion recovery technique

at frequencies of 100 MHz (^1H) and 25.14 MHz (^{13}C). Results are given in Table 7. Distinct ^{13}C resonances in the proton decoupled spectra were assigned via the additivity coefficients found²⁹ for alkanes with the assumption that the relaxation times decrease towards the chain centre. The value of T_1 for an interior methylene carbon was estimated by linearly extrapolating $\log T_1$ against $1/n$ to $1/n = 0$.

The solubility limit of heptane in poly(ethylene oxide) homopolymer of molecular weight $\bar{M}_n = 2000$ is about 0.08 volume fraction³⁰. The volume fraction of end-groups in a liquid sample of 7-45-7 is about 0.10^{24,25}, and the connectivity of the chain will increase the mutual solubility of the oxyethylene and methylene blocks. Hence we can be sure that the melt of sample 7-45-7 will be homogeneous, and that the values of T_1 recorded for this sample will be those

characteristic of a local environment of mixed oxyethylene and methylene chains. Comparison with the values of T_1 found for octadecane support this view. The values of T_1 found for sample 18-45-18 are practically identical with those found for sample 7-45-7 and so lend support to the view that the melt of sample 18-45-18 is homogeneous. This conclusion is in keeping with the SAXS results for the molten polymers.

DISCUSSION

Crystal structure

The SAXS and Raman scattering results show that the basic crystalline structure of all our samples is stacked lamellae which can be characterized as either extended or folded. The WAXS and d.s.c. results show that only the oxyethylene units crystallize. Moreover it is clear (WAXS) that they do so in the usual 7:2 helical conformation. There seems to be no doubt, and the n.m.r. results for the solid polymers (Figure 1) lend support to this view, that the methylene chains of the end-groups are in disordered layers which alternate with crystalline layers in the stacked structure.

The crystallinities which can be derived from the picnometric and d.s.c. results, and also the n.m.r. results for the solid polymers, are consistent with the presence in the disordered layers of a significant proportion of the oxyethylene chain units. A simple two phase model (i.e. perfect crystal plus perfect liquid with negligible excess surface quantities), used in conjunction with the picnometric (Table 3) and the d.s.c. (Table 4) data, leads to the estimates of the fractional crystallinity of the oxyethylene block ($X = \Delta v/\Delta v^0$ or $\Delta h/\Delta h^0$) which are listed in Table 8. The agreement between the values calculated from the two kinds of experimental data is satisfactory.

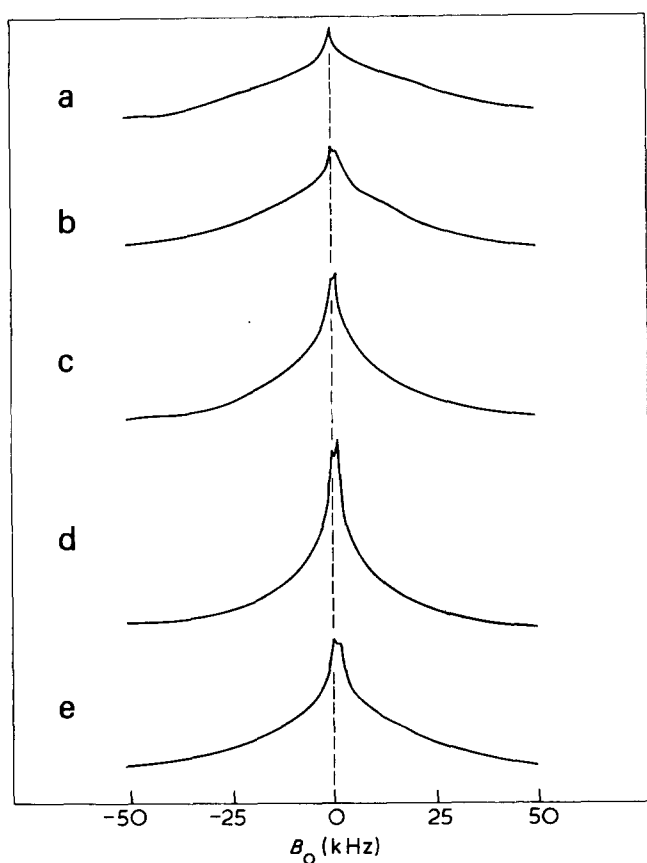


Figure 1 300 MHz proton magnetic resonance spectra of samples: (a) 0-45-0; (b) 4-45-4; (c) 7-45-7; (d) 10-45-10; (e) 18-45-18. Crystallization temperature was 25°C; spectra were recorded at 20°C. The zero of the abscissa corresponds to the mobile oxyethylene absorption

Table 6 N.m.r. assessment of mobile protons in solid polymers at 20°C

Sample	P
0-45-0	0.03
1-45-1	0.02
2-45-2	0.02
3-45-3	0.04
4-45-4	0.04
7-45-7	0.08
10-45-10	0.11
12-45-12	0.12
18-45-18	0.08

Table 7 N.m.r. spin lattice relaxation times at 60°C

Sample	T_1 (sec)									
	^{13}C resonance				^1H resonance					
	Methylene		Oxyethylene		Methylene		Oxyethylene			
	1	2	3	4	5	6	Int			
7-45-7	3.9	1.9	1.3	0.92	0.86	0.72	0.55	0.60	0.46	0.46
18-45-18	—	—	—	—	—	—	0.50	0.65	0.46	0.49
Octadecane	5.3	4.0	3.0	—	—	—	1.6	—	1.03	—

Table 8 Crystallinity of the oxyethylene block

Crystal type	x	
	Picnometry	D.s.c.
Two-phase model:		
Extended-chain	0.85	0.85
Once-folded chain	0.65	0.70
Buckley and Kovacs model:		
Extended-chain	—	0.85
Once-folded chain	—	0.70
Ashman and Booth model:		
Extended-chain	0.68	—
Once-folded chain	0.78	—

Enthalpy of fusion

An interesting feature of our results is the constant value of the enthalpy of fusion per gram of oxyethylene for a given type of crystal. A component of the enthalpy of fusion is the enthalpy of mixing of the methylene chains, which are partly segregated in the surface layers of the crystalline lamellae, with the oxyethylene chains. We have discussed this elsewhere¹⁶. For complete segregation of end-groups, which represents an upper limit to the effect, the enthalpy of mixing per gram of oxyethylene can be written (see Appendix II):

$$\Delta h_{\text{mixing}} = RT\chi_H\phi_{me}/44 \quad (1)$$

where ϕ_{me} is the volume fraction of the methylene blocks and χ_H is the Flory–Huggins enthalpy parameter for interaction of methylene and oxyethylene chain units. If we set $\chi_H = 0.7^{16,30}$, we find $\Delta h_{\text{mixing}} \sim 13$ J/g for sample 12-23-12, which has the largest value of ϕ_{me} (0.31) of the samples studied by d.s.c. If the end-groups are randomly mixed with oxyethylene groups in the disordered layer then the corresponding value of Δh_{mixing} for sample 12-23-12 ($\phi_{me} = 0.31$, crystallinity = 0.8) is (see Appendix II) $\Delta h_{\text{mixing}} \sim 7$ J/g. Thus we see that the mixing effect is small compared to the total heat of fusion (probably <5%) and is not discernible within our experimental errors.

Models of the solid polymer

The two phase model is unlikely to be correct for our systems, in which the disordered polymer is intimately associated with the ordered polymer. In considering other models the possible effect of the distribution of chain lengths in the crystallizable oxyethylene blocks must be borne in mind.

Buckley and Kovacs^{8,9} have pointed to the evidence for molecular segregation during the crystallization of low molecular weight poly(ethylene oxide)^{1,31} and have used a model in which chain ends and folds are paired in the surface layers of crystalline lamellae of variable thickness. The surfaces have constant (*MWD* independent) properties. For example the heat of fusion measured in J/(mol of oxyethylene units) of a sample of average chain length \bar{x}_n units with an average of t crystalline sequences per molecule is:

$$\Delta H(T) = \Delta H^0(T) - 2t\Delta H_f^e/\bar{x}_n \quad (2)$$

where ΔH^0 is the thermodynamic heat of fusion (of an infinitely large perfect crystal) and ΔH_f^e is the excess heat of

fusion of the real crystal measured in J/(mol of chains emerging). Non-integral values of t are possible if extended- and folded-chain lamellae both exist in the sample. In particular if the stacks consist of a random mixture of extended- and folded-chain lamellae³¹ t can be calculated from the LAXS results. The data of Table 2 yield $t \sim 1.7$ for the folded-chain crystals of series 34 and 45. (We discount series 23 here since we are wary of fractionation effects.) For most purposes we can set $t = 2$ for the folded-chain crystals. Taking $\Delta H^0(54^\circ\text{C})$ to be 8.8 kJ/mol (corresponding to 200 J/g: see earlier) and using the values from Table 4 of $t = 1$, $\Delta H(54^\circ\text{C}) = 7.48$ kJ/mol and $t = 2$, $\Delta H(54^\circ\text{C}) = 6.16$ kJ/mol we obtain for series 45 $\Delta H_f^e = 30$ kJ/(mol of chains emerging) independently of t . This result, that ΔH_f^e is not greatly dependent on the nature (all cilia, mixed cilia and folds) of the surface layer, is unexpected for the model.

The crystalline fractions predicted by assuming, following Buckley and Kovacs, that the enthalpy of a chain unit in the non-crystalline surface layer is equal to that in the melt are necessarily equal to those calculated earlier from the d.s.c. data. The point is made in Table 8.

Ashman and Booth¹⁸ have assumed complete molecular mixing during crystallization (except for those systems in which there are overt signs of fractionation) so that all chains are accommodated, extended or folded as appropriate, within lamellae of uniform thickness. In this model a disordered layer contains end-groups and folds at various depths, and the thickness of the disordered layer is influenced by the distribution of oxyethylene block lengths. With some assumptions concerning the extent of chain-folding^{18,19} this model has been used to characterize the solids formed from oxyethylene homopolymers and oxyethylene–oxypropylene block copolymers. Applying similar techniques to our present data (*MWD*, *SAXS*, v_{sp}) we find results which parallel in most respect those presented earlier^{18,19}; in particular we find that the crystalline fraction is lower in the extended-chain crystals than in the folded-chain crystals (see Table 8) for which t is approximately 1.7. The values of X differ from those calculated from picnometric data by means of the two phase model (Table 8) because the Ashman model allows the specific volume of the polymer in the disordered layer to be evaluated (rather than requiring it to be identical with that of the melt), and we find the ratio of the specific volume of the material in the disordered layer to that of melt of the same composition to be about 0.97 for the extended-chain systems and about 1.02 for the folded-chain systems.

These results can be reconciled with the d.s.c. results (Table 4) only if the enthalpy of formation of melt from the disordered layer is much larger for an extended-chain solid than for a folded-chain solid. We can regard the low specific volume and enthalpy of the disordered layers of the extended chain crystals as a manifestation of partial crystallization within the layer and this amounts to a reconciliation with the Buckley and Kovacs model. We find no such reconciliation between the two models for the folded-chain crystals.

In our discussion of the melting points (which follows) we will simply assume an alternating layer model in which the disordered layers comprise the complete methylene blocks plus 20% of the oxyethylene blocks.

Melting points

In Figure 2 we plot melting points (averaged values, ± 1 K) against the number of methylene units in the end-group (n). For the extended-chain crystals (Figure 2a) T_m is broadly independent of n in the range $n = 0$ to 5. For the folded-

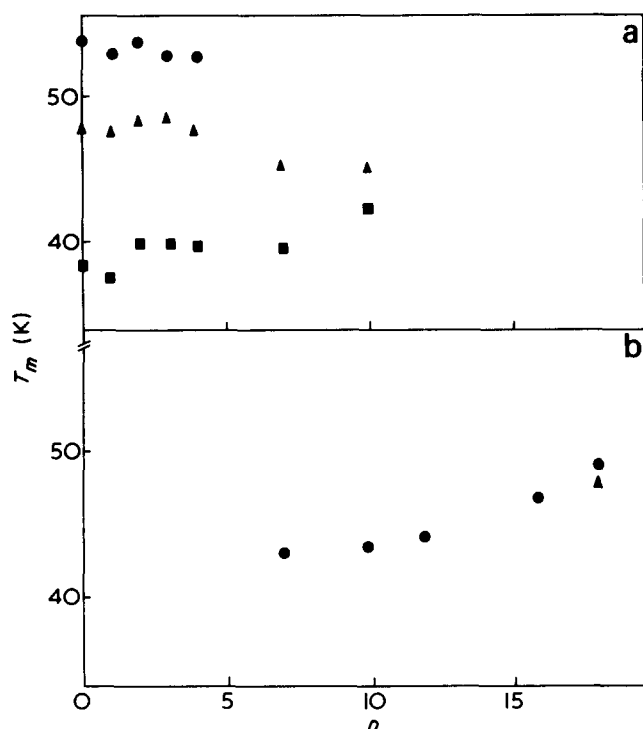


Figure 2 Effect of methylene chain length (n) on melting point of (a) extended-chain crystals; (b) folded-chain crystals. The assignment to (a) or (b) is on the basis of the LAXS results of Table 2. Melting points are averaged values taken from Table 5: ■, series 23; ▲, series 34; ●, series 45

chain crystals (Figure 2b) T_m increases as n increases in the range $n = 7$ to 18. (The high values of T_m obtained for samples 18-23-18 and 18-34-18 crystallized at 45°C are omitted from the plots.) We cannot explain the erratic dependence of T_m on n for $n > 5$ in Figure 2a. However, we place most reliance on the melting points obtained for series 45, for which we have duplicate samples, and it is these results which we compare with calculations in Figure 3.

For our polymers the melting point can be related to structural variables via the Flory-Vrij equation^{18,32}:

$$T_m = T_m^0 \{1 - 2\sigma_e / \Delta H^0 l_c\} / \{1 - RT_m^0 \ln(\phi_{oe} l) / \Delta H^0 t l_c\} \quad (3)$$

in which the only symbols yet undefined are T_m^0 , the thermodynamic melting point of poly(ethylene oxide); σ_e , the end interfacial free energy of the crystalline lamellae (i.e. the free energy of formation from the melt of the disordered layer and the disordered/crystalline interface); l_c , the thickness of the crystalline lamellae (in chain units); and l , the combinatorial entropy parameter for the crystal (i.e. effectively the probability that a sequence of l_c chain units is entirely composed of oxyethylene units^{32,33}).

In this discussion we shall assume that for a given type of crystal (extended or folded) formed from samples containing a given oxyethylene block (23, 32, or 45 units) the crystalline lamella thickness (l_c) is constant. This is in keeping with the picnometric and d.s.c. results. We shall also assume that the folding parameter is either $t = 1$ (extended) or $t = 2$ (once-folded) for our samples. With these assumptions l is

constant for a given series (i.e. for a given MWD of the oxyethylene block) and so, since T_m^0 and ΔH^0 are constants for the oxyethylene chain, the only variables which influence the relative values of T_m , within a series of samples, are ϕ_{oe} and σ_e .

The end interfacial free energy σ_e can be written:

$$\sigma_e = \sigma_0 + \sigma_d \quad (4)$$

where σ_0 is the free energy of formation from the melt of the crystal-non-crystal interface (i.e. a term due to the imbalance of intermolecular interaction at the interface), and σ_d is the free energy of formation from the melt of the non-crystalline layer. This latter contribution can itself be written:

$$\sigma_d = \sigma_m + \sigma_a \quad (5)$$

where σ_m is the free energy change (enthalpy and non-combinatorial entropy changes) due to concentration, relative to the melt, of methylene units in the disordered layer, and σ_a is the free energy increase due to conformational restrictions, relative to the melt, of the chains in the disordered layer. We assume hereafter that σ_0 is constant for the samples of a given series. We justify this by recalling that some 20% of the oxyethylene units are in the disordered layer so that the crystal/non-crystal interface is probably best regarded as an ordered poly(ethylene oxide)/disordered poly(ethylene oxide) interface. In what follows we examine the effect upon T_m of variation of ϕ_{oe} , σ_a and σ_m .

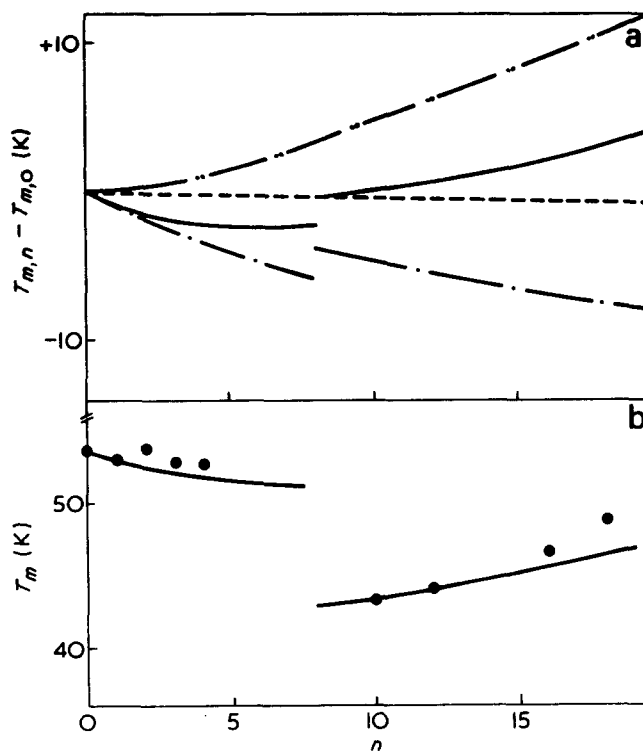


Figure 3 Effect of methylene chain length (n) on melting points of series 45. (a) Contributions to $T_{m,n} - T_{m,0}$ from dilution (---), conformational restriction (-·-·-) and mixing (·····) together with the combined effect (—). (b) Comparison of experimental melting points (●) with those calculated as described in the text (—)

Effect of dilution: ϕ_{oe} . Equation (3) can be written:

$$T_m = \frac{1}{\alpha - \beta \ln \phi_{oe}} \quad (6)$$

where

$$\alpha = (1 - RT_m^0 \ln l / \Delta H^0 l_c) / T_m^0 (1 - 2\sigma_e / \Delta H^0 l_c) \quad (7)$$

and

$$\beta = R / [\Delta H^0 l_c (1 - 2\sigma_e / \Delta H^0 l_c)] \quad (8)$$

Differentiation with respect to ϕ_{oe} gives:

$$(dT_m / d\phi_{oe}) = \beta T_m^2 / \phi_{oe} \quad (9)$$

whence, the increase in T_m consequent upon an increase in ϕ_{oe} is:

$$\Delta T_m = \beta T_m^2 \Delta \phi_{oe} / \phi_{oe} \quad (10)$$

For any reasonable value of σ_e

$$\beta \sim R / \Delta H^0 l_c \sim 10^{-3} / l_c \sim 10^{-3} / \bar{x}_n \quad (11)$$

where \bar{x}_n is the average chain length of the oxyethylene block. Thus for small values of ϕ_{oe} the difference in melting point between hydroxy-ended ($T_{m,0}$) and alkoxy-ended ($T_{m,n}$) samples due to the dilution effect is:

$$T_{m,n} - T_{m,0} \sim -10^{-3} T_{m,0}^2 (1 - \phi_{oe}) / \bar{x}_n \quad (12)$$

Effect of conformation restriction: σ_a . Equation (3) can be written:

$$T_m = \gamma T_m^0 (1 - 2\sigma_e / \Delta H^0 l_c) \quad (13)$$

where

$$\gamma = [1 - RT_m^0 \ln(l\phi_{oe}) / \Delta H^0 l_c]^{-1} \quad (14)$$

Consequently the difference in melting point between hydroxy-ended and alkoxy-ended samples due to the conformational effect is

$$T_{m,n} - T_{m,0} = \delta (\sigma_{a,0} - \sigma_{a,n}) \quad (15)$$

where $\delta = 2\gamma T_m^0 / \Delta H^0 l_c$ is a constant. The evidence we have from our work with oxyethylene/oxypropylene block copolymers^{18,19}, for which mixing effects are small, is that σ_a varies as the logarithm of the emerging chain length. This result is in conformity with theoretical predications³⁴⁻³⁶. Consequently we write:

$$T_{m,n} - T_{m,0} = (\epsilon/t) \log_{10}(n'/n' + n) = (\epsilon/t) \log_{10}(1 + n/n') \quad (16)$$

where n' is the length (in chain atoms) of the oxyethylene component of the emerging chain and ϵ is the appropriate constant of proportionality. For series 45 with $X = 0.8$, i.e. $n' = 14$, the melting point results for type PEP copolymers (Table 2 of Ref 19) are roughly consistent with $\epsilon = 30\text{K}$ (extended-chain) or $\epsilon = 40\text{K}$ (folded-chain).

Effect of mixing: σ_m . The n.m.r. and SAXS results for the molten polymers are consistent with homogeneous melts and so we rule out of consideration aggregation (micellization) in the melt. We further assume that the melt and the disordered layer are random mixtures of oxyethylene and methylene chains, whence conventional polymer mixing theory leads (see Appendix II) to the expression:

$$\sigma_m = -RT\chi(1 - \phi_{oe})^2 l_c / 2(1 - X\phi_{oe}) \quad (17)$$

where χ is the Flory-Huggins interaction parameter for the system based on a segment volume equal to that of an oxyethylene unit in the melt. Assuming that the oxyethylene and methylene chains have similar equations of state we can approximate χ by χ_H , the enthalpy parameter, for which we have the value of 0.7^{16,30}. Introduction of σ_m into equation (13) with γ approximated by unity (which is sensible for any reasonable value of l) gives:

$$T_m \sim T_m^0 (1 - 2\sigma_m / \Delta H^0 l_c) \quad (18)$$

Consequently the difference in melting point between hydroxy-ended and alkoxy-ended samples due to mixing effects is:

$$T_{m,n} - T_{m,0} \sim RT_{m,0}^2 (1 - \phi_{oe})^2 / \Delta H^0 (1 - X\phi_{oe}) \quad (19)$$

where we use $T_{m,0} \sim T_m^0$.

Overall effect and comparison with experiment

In Figure 3a the three contributions to $T_{m,n} - T_{m,0}$ which can be estimated for the samples of series 45 are plotted separately and also combined to illustrate the overall effect of oxyethylene chain extension by methylene chains. In Figure 3b we use $T_{m,0} = 53.6^\circ\text{C}$ (extended-chain crystals) and $T_{m,0} \sim 43^\circ\text{C}$ (estimated for folded-chain crystals; in Figure 3a $T_{m,n} - T_{m,0} \sim 0\text{K}$ for $n = 10$) to compare measured and calculated melting points for the series 45. The rough agreement between the two results is justification of our treatment of the effects.

ACKNOWLEDGEMENTS

We thank Mr D. J. Roy, Mr A. Redfern and Mr J. J. Smith for technical assistance; Dr R. H. Mobbs and Mr R. L. Beddoes for helpful advice; and the Science Research Council for financial support (D.R.C., Y.-K.L.) and for provision of facilities for the nuclear magnetic resonance spectroscopy.

REFERENCES

- 1 Arlie, J. P., Spegt, P. A. and Skoulios, A. E. *Makromol. Chem.* 1966, **99**, 160
- 2 Arlie, J. P., Spegt, P. A. and Skoulios, A. E. *Makromol. Chem.* 1967, **104**, 212
- 3 Spegt, P. A. *Makromol. Chem.* 1970, **140**, 167
- 4 Beech, D. R., Booth, C., Dodgson, D. V., Sharpe, R. R. and Waring, J. R. S. *Polymer* 1972, **13**, 73
- 5 Ashman, P. C. and Booth, C. *Polymer* 1972, **13**, 459
- 6 Kovacs, A. J. and Gonthier, A. *Kolloid-Z* 1972, **250**, 530
- 7 Kovacs, A. J., Gonthier, A. and Straupe, C. J. *Polym. Sci. Polym. Symp.* 1975, **50**, 283
- 8 Buckley, C. P. and Kovacs, A. J. *Prog. Colloid Polym. Sci.* 1975, **58**, 44
- 9 Buckley, C. P. and Kovacs, A. J. *Colloid Polym. Sci.* 1976, **254**, 695

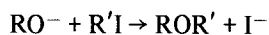
- 10 Hartley, A. J., Leung, Y.-K., Booth, C. and Shepherd, I. W. *Polymer* 1976, **17**, 354
- 11 Hartley, A. J., Leung, Y.-K., McMahon, J., Booth, C. and Shepherd, I. W. *Polymer* 1977, **18**, 336
- 12 Mathis, A., Thierry, A., Terrisse, J. and Skoulios, A. *Makromol. Chem.* 1972, **158**, 205
- 13 Booth, C., Bruce, J. M. and Buggy, M. *Polymer* 1972, **13**, 475
- 14 Ashman, P. C. and Booth, C. *Polymer* 1973, **14**, 300
- 15 Fraser, M. J., Marshall, A. and Booth, C. *Polymer* 1977, **18**, 93
- 16 Fraser, M. J., Cooper, D. R. and Booth, C. *Polymer* 1977, **18**, 852
- 17 Booth, C. and Pickles, C. J. *J. Polym. Sci. (Polym. Phys. Edn)* 1973, **11**, 249
- 18 Ashman, P. C. and Booth, C. *Polymer* 1975, **16**, 889
- 19 Ashman, P. C., Booth, C., Cooper, D. R. and Price, C. *Polymer* 1975, **16**, 897
- 20 Cooper, D. R. and Booth, C. *Polymer* 1977, **18**, 164
- 21 Friday, A., Cooper, D. R. and Booth, C. *Polymer* 1977, **18**, 171
- 22 'Polymer Handbook', 2nd Edn (Eds J. Brandrup and E. H. Immergut) Interscience, New York, 1975
- 23 Olf, H. G., Peterlin, A. and Peticolas, W. L. *J. Polym. Sci. (Polym. Phys. Edn)* 1974, **12**, 359
- 24 Simon, F. T. and Rutherford, J. M. *J. Appl. Phys.* 1964, **35**, 83
- 25 Flory, P. J., Eichinger, B. E. and Orwoll, R. A. *Macromolecules* 1968, **1**, 287; Orwoll, R. A. and Flory, P. J. *J. Am. Chem. Soc.* 1967, **89**, 6814
- 26 Roberts, R. C. *PhD Thesis* University of Manchester (1966)
- 27 Devoy, C. J. *PhD Thesis* University of Manchester (1966)
- 28 Booth, C., Devoy, C. J. and Gee, G. *Polymer* 1971, **12**, 327
- 29 Grant, D. M. and Paul, E. G. *J. Am. Chem. Soc.* 1964, **86**, 2984
- 30 Leung, Y.-K. *Polymer* 1976, **17**, 374
- 31 Gilg, B. and Skoulios, A. E. *Makromol. Chem.* 1970, **140**, 149
- 32 Flory, P. J. and Vrij, A. *J. Am. Chem. Soc.* 1963, **85**, 3548
- 33 Flory, P. J. *J. Chem. Phys.* 1949, **17**, 273
- 34 DiMarzio, E. A. *J. Chem. Phys.* 1965, **42**, 2101
- 35 McCrackin, F. L. *J. Chem. Phys.* 1967, **47**, 1980
- 36 Bellemans, A. *J. Polym. Sci. (C)* 1972, **39**, 305
- 37 Flory, P. J. 'Principles of Polymer Chemistry', Ithaca, New York, 1953

APPENDIX I

Alkoxylation of α,ω -hydroxy-poly(ethylene oxide)

The methoxylation of α,ω -hydroxy-poly(ethylene oxide) has been described elsewhere²⁰. The same type of Williamson synthesis was used for the higher alkoxides: changes in method are noted below.

For alkyl halides with β -hydrogen atoms the nucleophilic substitution reaction:



is accompanied by an elimination reaction:



Large molar excesses of hydroxide (50-fold) and iodide (4 to 8-fold) serve to compensate for losses by this route.

Chlorobenzene was used as solvent. Solid octadecyl iodide was dissolved in a little chlorobenzene before addition to the reaction mixture.

Rotary evaporation at temperatures below 60°C served to remove the bulk of the excess heptyl and lower iodides. Higher alkyl iodides were removed by washing and recrystallization.

The dichloromethane phase resulting from the washing procedure was sometimes coloured by traces of iodine. This was removed with active charcoal at this and, if necessary, at later stages.

The solid residue from the dichloromethane phase was

taken up in dry benzene, cooled in ice, and precipitated by adding a 10-fold volume excess of isooctane. The crystals were removed by filtration (G4 sinter). This crystallization process was repeated until the supernatant liquid was free of iodide (silver nitrate test). Samples 10-23-10 and 12-23-12 proved difficult to recrystallize in this way: they were dissolved in hot isooctane and precipitated therefrom at 0°C.

The samples were finally dried by evacuation (<1 Pa) of the melt at 70°C for several days.

APPENDIX II

Non-combinatorial contributions to the free energy of crystal formation

The combinatorial entropy of mixing of end and chain segments is included in the Flory-Vrij treatment of crystal formation³². Here we compute the non-combinatorial contribution to the free energy of formation from the melt of the disordered layers of the stacked lamella crystal.

Let the average number of oxyethylene segments per chain be r_{oe} and the corresponding number of methylene segments be r_{me} . (The segment size is (arbitrarily) identified with that of the oxyethylene unit.) In terms of the volume fraction of oxyethylene, assuming negligible volume changes on mixing,

$$r_{me} = r_{oe}(1 - \phi_{oe})/\phi_{oe} \quad (\text{A1})$$

If the fraction X of the oxyethylene segments crystallize then the number of disordered segments per chain is $r_{oe}(1 - X) + r_{me}$ and the volume fraction of oxyethylene in the disordered layer is:

$$\phi_{oe}' = (1 - X)/[(1 - X) + (1 - \phi_{oe})/\phi_{oe}]$$

With these definitions, and assuming random mixing in both melt and disordered layer, the non-combinatorial free energy of mixing oxyethylene and methylene per mole of chains in the melt is³⁷

$$\Delta G_1 = RT\chi\phi_{oe}(1 - \phi_{oe})(r_{oe}/\phi_{oe}) = r_{oe}RT\chi(1 - \phi_{oe}) \quad (\text{A2})$$

and the corresponding free energy of mixing per mole of chains in the disordered layer is:

$$\Delta G_2 = r_{oe}RT\chi(1 - X)(1 - \phi_{oe})/\phi_{oe} [(1 - X) + (1 - \phi_{oe})/\phi_{oe}] \quad (\text{A3})$$

Hence the non-combinatorial free energy change on forming the disordered layer from the melt is:

$$\Delta G = \Delta G_2 - \Delta G_1 = -r_{oe}RT\chi(1 - \phi_{oe})^2X/(1 - X\phi_{oe}) \quad (\text{A4})$$

If the oxyethylene and methylene chains are completely segregated in the disordered layer but randomly mixed in the melt then:

$$\Delta G = -r_{oe}RT\chi(1 - \phi_{oe}) \quad (\text{A5})$$

The assumption that the non-combinatorial entropy contri-

bution is small compared to the enthalpic contribution, together with division by $44r_{oe}$ to obtain the free energy per gram of oxyethylene, leads to equation (1).

For the case of random mixing in the disordered layer the contribution of mixing to the free energy of formation of the disordered layer from the melt which we have called σ_m is given by:

$$\sigma_m = \Delta G/2t = -r_{oe}RT\chi(1 - \phi_{oe})^2X/2t(1 - X\phi_{oe}) \quad (\text{A6})$$

where the factor $2t$ (t being the average number of crystalline sequences per chain) converts to the free energy contribution *per mole of chains emerging from the crystalline layer into the disordered layer*. Since $l_c = r_{oe}X/t$, equation (A6) is identical with equation (17).